Synthesis of Negative Resistance Reflection Amplifiers Employing Band-Limited Circulators

H. C. OKEAN, MEMBER, IEEE

Abstract—This paper presents a theory for single-stage circulator-coupled negative resistance reflection amplifiers based on proposed realistic circuit models for frequency-dependent band-limited circulators and broadband negative resistance devices such as the tunnel diode. In particular, gain bandwidth limitations are derived which are imposed by both the inherent resonance associated with the nonreciprocal circulator junction and the reactive parasitics associated with the active device. These limitations are generally more restrictive than past results which assumed a "perfect" frequency-independent circulator and took into account only the device parasitics. In addition, a synthesis procedure is presented for realization of an absolutely stable amplifier with a prescribed nth-order Butterworth or Chebyscheff approximation to an ideally flat band-pass power gain characteristic.

The approach employed is based upon the theory of reflection coefficient equalization between two reactively constrained resistances representing the pass band circulator and device immittance models. In addition, a band rejection out-of-band stabilizing network is absorbed in the pass band equalizer in accordance with an overall synthesis procedure.

Finally, the theory is verified by the construction and testing of an L-band tunnel diode amplifier having third-order maximally flat power gain centered at 1.46 Gc/s and with half-power bandwidths (430 Mcls and 355 Mc/s at 10 dB and 16dB midband gain) within six percent of those predicted by theory.

I. Introduction

THE CIRCULATOR-COUPLED reflection amplifier has been found to be the optimum single-stage negative resistance amplifier configuration at microwave frequencies [1], particularly with respect to noise performance and insensitivity to source and load impedance variations. It consists of a three-port circulator terminated in source, load, and negative resistance network such that the incident RF wave from the source is amplified at, and reflected from, the negative resistance port and transmitted to the load. The nonreciprocity of the circulator separates the incident and the reflected waves.

This paper is concerned with the development of a theory for single-stage circulator-coupled negative resistance band-pass reflection amplifiers based upon realistic circuit models for frequency-dependent circulators and broadband one-port negative resistance devices. Past theoretical treatment of such amplifiers [2]–[11] generally postulated a "perfect" frequency-independent circulator and considered only the limitations imposed by the parasitics of the active device, although the perturbing effects of small, frequency-independent circulator imperfections have been considered [12], [13]. The perfect circulator assumption yielded overly optimistic predictions of amplifier gain-bandwidth capabilities, particularly for broadband active devices such as the tunnel diode. This is borne out by the measured gain-frequency characteristics of practical tunnel diode amplifier designs [14]–[20] which fall short of their predicted bandwidth capabilities or display unwanted pass band gain ripples. Furthermore, stabilization of the active device in the face of uncontrolled out-of-band circulator behavior was, with rare exception [2], [6], overlooked in the theoretical studies but usually found necessary in practical designs.

Therefore, this paper formulates the gain-bandwidth limitations imposed upon a circulator-coupled negative resistance reflection amplifier by the frequency dependence of both realistic circulator and active device circuit models. This in turn leads to a synthesis procedure for a network interposed between active device and circulator which realizes an absolutely stable amplifier with a precisely specified band-pass power gain characteristic. The approach employed consists of two steps: pass band gain equalization and out-of-band stabilization. Finally, data is presented on an experimental L-band tunnel diode amplifier which verifies the theory.

A list of principal symbols and nomenclature used in this paper is presented in Table I.

II. Establishment of Circuit Models

A. Reflection Amplifier Configuration

The general circulator-coupled negative resistance amplifier configuration is shown in Fig. 1. The overall coupling network N_T interposed between circulator and active device consists, basically, of a cascade of lossless transducer-transformer network N_x and equalization-stabilization network N. N_x transforms between different circulator and device transmission media and/or impedance levels (R_0 and R_n), whereas N is restricted to be essentially lossless in the amplifier pass band in order not to degrade the amplifier noise performance.

Let the circulator be characterized by a pass band

Manuscript received October 14, 1965; revised April 6, 1966. This paper is based upon a dissertation submitted by the author in partial fulfillment of the requirements for the Eng.Sc.D. degree in the Department of Electrical Engineering at Columbia University, New York, N. Y. The research was supported in part by the U. S. Army Ordnance Department under Contract DA-30-069-ORD-1955.

The author is with Bell Telephone Laboratories, Inc., Murray Hill, N. J.

TABLE I

PRINCIPAL SYMBOLS AND NOMENCLATURE

Symbol	
R_0, R_n	Circulator, transformed circulator impedance level
$W(\omega)$	Overall insertion power gain function
$W_A(\omega)$	Reflection gain at negative resistance port of circulator
ρ_A, ρ_A'	Reflection coefficients at negative resistance port
S, s', s'', s'''	Symmetrical circulator scattering matrix and elements
Y_c', Y_c	Circulator, transformed circulator input admittance
$\omega_0 = 2\pi f_0$	Amplifier center frequency
η	Band-pass frequency variable
$\Delta Z_c'$, ΔZ_c	Circulator, transformed circulator deviation impedance
N_x, N	Transformer and equalizer-stabilizer networks
L, C_p, R_s, C, $-R$	Small signal tunnel diode parameters
N_1, N_0, N_n	Active band-pass (ABP) prototype two-ports
N_{1L}, N_{0L}, N_{nL}	Passive low-pass (PLP) prototype two-ports
$\pm R_1$, R_n	ABP and PLP terminations
ρ_1, ρ_n, ρ_{A1}, ρ_{An}	PLP and ABP reflection coefficients
p_{0i}, p_{pi}	Poles and zeros of $\rho_1(p)$ in $p = \sigma + j\omega$
Q_d, Q_d', q_c, q_c'	Device and circulator constraining selectivities
ω_{01}, ω_{01}', ω_{0n}, ω_{0n}'	PLP reactive constraining elements
ω_c, w_c, w	Frequency scaling parameters
γ_j, q_j	PLP, ABP prototype ladder element values ($j = 1, 2, \cdots, n$)
β	Amplification bandwidth, normalized to ω_0
$H = U + jV$	Immittance (impedance or admittance)
P	Number of poles in p of $H(p)$ with Re $(p) \geq 0$
β_{s0}	Stability bandwidth, normalized to ω_0
U_{0s}, U_{st}	Stabilizing network conductances or resistances
$\bar{q}_{st}$, $\bar{q}_{js}$	Stabilizing network selectivities ($j = 1, 2, \cdots, m_t$)
R_{Ls}, G_{Lp}	Loss resistance, conductance

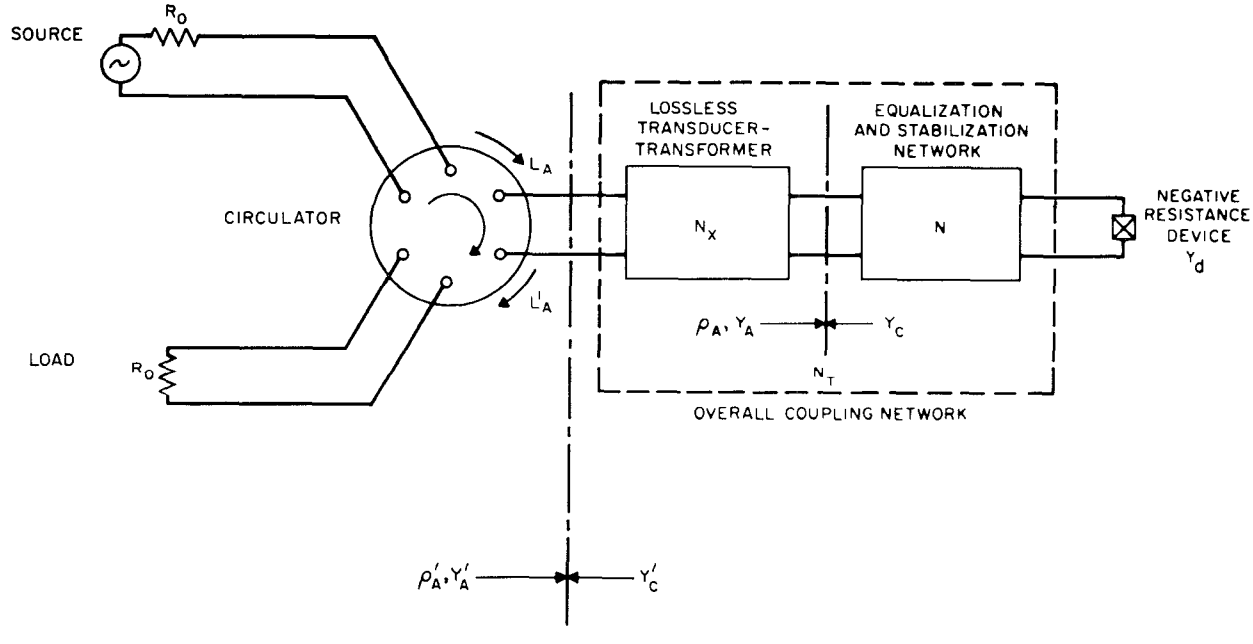

Fig. 1. Circulator-coupled, negative resistance reflection amplifier configuration.

centered at frequency f_0 over which its cyclically symmetric forward and reverse transmission and input reflection scattering matrix elements s'', s''', and s' [13] approach those of a "perfect" circulator ($s'=s'''\equiv 0$, $s''\equiv 1$), such that

$$|s''| \lesssim 1, \qquad |s'|, \qquad |s'''| \ll 1.$$

Then, the overall insertion power gain $W(f)$ of a reflection amplifier having a pass band within that of the circulator and centered at f_0 may be accurately represented in the amplifier pass band by

$$W(f) \cong |s''|^4 W_A = |s''|^4 |\rho_A(j\omega)|^2 \tag{1}$$

where

$$\rho_A = \frac{Y_C^* - Y_A}{Y_C + Y_A} \text{ at interface of } N_x \text{ and } N$$
$$|\rho_A| \gg 1 [R_e(Y_A) < 0].$$

The total circulator forward transmission $|s''|^4 \lesssim 1$ is relatively constant over the circulator pass band so that the amplifier synthesis problem, realization of a prescribed $W(f)$, is accomplished by the synthesis of network N for a particular $|\rho_A|^2$. Similarly, amplifier gain-bandwidth limitations are those imposed on $|\rho_A(j\omega)|^2$ by both $Y_C(j\omega)$ and $Y_A(j\omega)$, rather than just by $Y_A(j\omega)$ as in the perfect circulator case ($Y_C'=R_0^{-1}$, $Y_C=R_n^{-1}$). Finally, precise reflection amplifier synthesis for specified $\overline{W}_A$, $\bar{\rho}_A'$ usually precludes the approximation of a band limited circulator by a "perfect" circulator ($s'=0$) under which the actual gain W_A is sufficiently perturbed [16] to introduce pass band gain ripple r, given by

$$r \le r_M = \frac{W_{A\max}}{W_{A\min}} = \left(\frac{1+|s'|\sqrt{\overline{W}_A}}{1-|s'|\sqrt{\overline{W}_A}}\right)^2;$$
$$W_A = \frac{\overline{W}_A}{|1 - s'\bar{\rho}_A'|^2} \tag{2}$$

as well as possible bandwidth degradation and/or out-of-band oscillation.

B. Circulator Representation

Recent theoretical and experimental characterizations of symmetrical three-port ferrite junction circulators [21]–[24] attribute a single-tuned frequency dependence to the scattering parameters and input immittance of the internal three-port ferrite junction in the circulator pass band centered at f_0. Lossless impedance level and/or transmission medium transformations in each circulator arm from the internal junction to the three external ports result in input immittance behavior at each external port which may be approximated in the circulator pass band by double-tuned circuit models [23], [24]. In particular, at the negative resistance port at the reference planes of either Y_C' or Y_C (Fig. 1), the pass band input immittance is representable, as shown in Fig. 2(a) and 2(b), by

$$Y_C'R_0 \quad \text{or} \quad \frac{Z_C'}{R_0} \approx \frac{1}{1+j\bar{q}_e\eta} + j\bar{q}_e'\eta \tag{3a}$$

$$Y_CR_n \quad \text{or} \quad \frac{Z_C}{R_n} \approx \frac{1}{1+jq_e\eta} + jq_e'\eta \tag{3b}$$

$$\eta = \frac{f}{f_0} - \frac{f_0}{f}. \tag{3c}$$

The selectivities q_e, $\bar{q}_e$, and q_e', $\bar{q}_e'$, attributable to the ferrite junction and to the internal and external transformation networks, respectively, may be readily obtained from measured immittance loci on a best fit basis.

The circuit models of Fig. 2(a) and 2(b) are made sufficiently general to represent Y_C' and Y_C at all frequencies by replacing R_0 and R_n by arbitrary deviation impedances $\Delta Z_C'$ and ΔZ_C which reduce to R_0 and R_n in the circulator pass band, and which may be obtained out of band from measured data on Y_C' and Y_C as shown in Fig. 2(c) and 2(d). Whereas the pass band approximations $\Delta Z_C' \cong R_0$, $\Delta Z_C \cong R_n$ are used in the pass band gain equalization, more general $\Delta Z_C'$ and ΔZ_C may be used to account for small pass band imperfections as well as for uncontrolled out-of-band circulator behavior in the out-of-band stabilization.

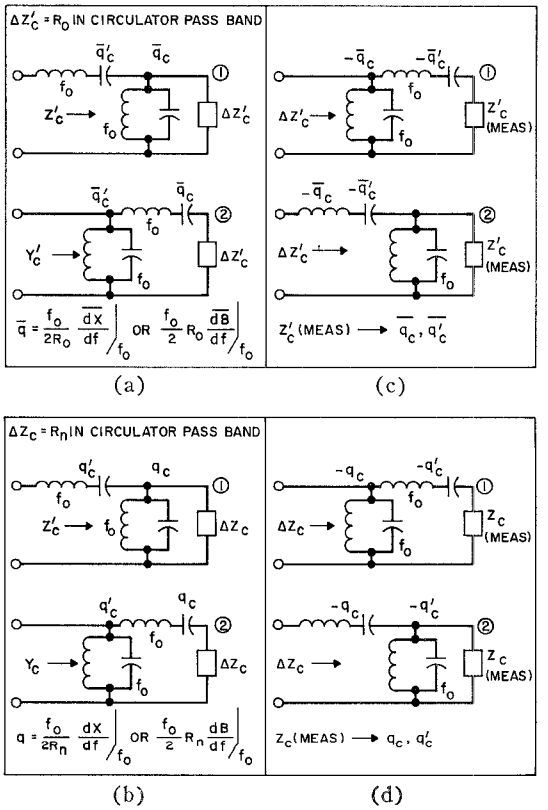

Fig. 2. (a), (b) Equivalent circuit models of circulator input immittance. (c), (d) Transformation networks for obtaining deviation immittance from measured data.

C. Negative Resistance Device Representation

Assuming linear small signal operation, a one-port "tuned" negative resistance device may generally be represented [7] by a constant negative resistor coupled to its external terminals through a network containing the reactive device parasitics, additional reactive tuning elements which resonate these at some f_0, and ohmic losses which restrict the "active" (negative resistance) range of the device to a finite frequency band $\Delta\omega_A$. This representation may be reduced, in the amplifier pass band centered about f_0, to that of a singly or doubly tuned negative resistor, as shown in Fig. 3, for use in the pass band gain equalization. For out-of-band stabilization, the exact device immittance is used, as obtainable from the pass band model by incorporating all out-of-band deviations in series and shunt deviation immittances (Fig. 3) which reduce to zero in the pass band.

The pass band models of the pumped maser element [9] and varactor diode [7] may both be approximated by Fig. 3(b). That of the suitably biased tunnel diode is obtained from its exact small signal equivalent circuit of Fig. 4 by adding appropriate shunt inductive and series capacitive tuning elements to resonate the diode parasitics at f_0. The resulting exact triple-tuned negative resistance model [11] reduces to either the single- or double-tuned pass band model of Fig. 3(a) and 3(b), respectively, depending upon whether $k=L/RCR_s$ is less than or greater than about 1.5, assuming $R_s \ll R$ and $f_0 \lesssim f_R/3$ where

$$f_R = \frac{1}{2\pi RC}\sqrt{(R/R_s)-1}$$

(Fig. 4). Alternatively, series-tuning [6] the diode (Fig. 4) by adding sufficient L and C_p to make $|G_{ED}|$ a maximum and B_{ED} zero at f_0, yields the somewhat less accurate pass band model of Fig. 3(d).

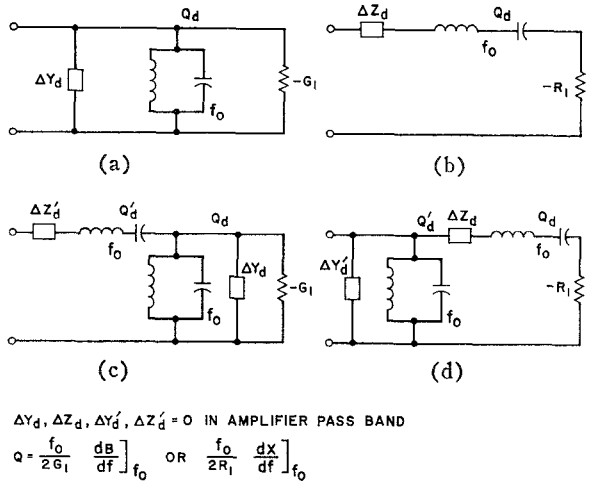

Fig. 3. Pass band small signal equivalent circuits for general negative resistance device.

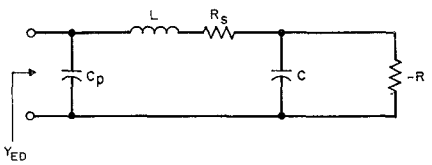

Fig. 4. Small signal equivalent circuit of tunnel diode.

III. Pass Band Gain Equalization

A. Formulation of the Problem

The pass band gain equalization problem consists of the determination of the limitations imposed by given pass band circulator and active device input immittance models on the realization of a specified gain $W_A(f)$, assuming a lossless two-port network interposed between them, and the development of a synthesis procedure for obtaining the pass band prototype of this network.

The problem is shown schematically in Fig. 5(a), in which the augmented[1] pass band models of the circulator and active device immittances are represented by lossless band pass constraint networks N_n and N_1 terminated in R_n and $-R_1$, respectively, and N_0 is the lossless pass band equalization network. Networks N_n and N_1, shown in detail in Fig. 6, each have, at most, two transmission zeros at ω_0. As stated, the problem is related to that of lossless reflection coefficient equalization between two reactively constrained positive resistances, as treated by Fielder [28], based upon earlier work by Bode [25], Fano [26], and Kinariwala [27]. To apply Fielder's results, which assume low-pass reactive constraining and matching networks, we employ an established [3], [7], [31] one-to-one correspondence between the active band pass configuration under consideration [R_n, N_n, N_0, N_1, $-R_1$; Figs. 5(a) and 6] and a passive low-pass prototype [R_n, N_{nL}, N_{0L}, N_{1L}, $+R_1$; Figs. 5(b) and 6] under restrictions imposed by losslessness, stability, and realizability.

B. Restrictions Upon General Lossless Equalization

The first step in the pass band gain equalization is the modification of a set of existing gain integrals [28] involving the passive low-pass reflection coefficients

$$|\rho_1(j\omega)| = |\rho_n(j\omega)| = \frac{1}{\sqrt{W_A}},$$

corresponding to W_A, the specified band pass reflection gain function. We decompose

$$|\rho_1(j\omega)|^2 = [\rho_1(p)\rho_1(-p)]_{p=j\omega}$$

such that all of the zeros p_{0i} and poles p_{pi} of $\rho_1(p)$ in complex frequency $p=\sigma+j\omega$ have Re (p_{0i}), Re $(p_{pi})<0$

[1] The augmented immittance representation is employed to insure that the first elements of N_0 at the N_1 and N_n interfaces are not required by the synthesis to be of the same type as the adjacent elements in N_1 and N_n, thereby avoiding degenerate transmission zeros in the $N_n+N_0+N_1$ cascade. Augmentation allows the selectivities of the resonators in N_n and N_1 adjacent to N_0 to be increased arbitrarily above those due to the pass band circulator and device models.

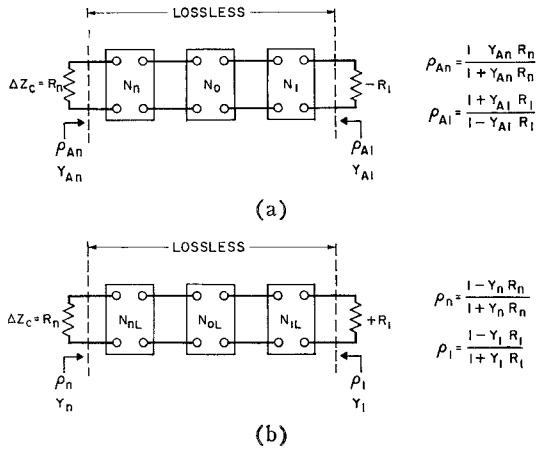

Fig. 5. Pass band reflection gain equalizer configurations. (a) Active band-pass model. (b) Passive low-pass model.

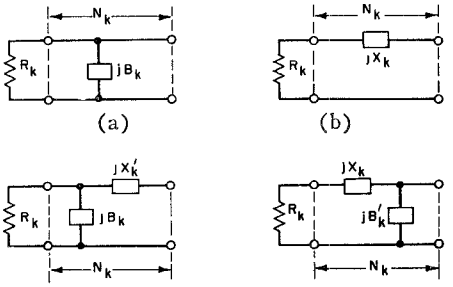

FIG		ACTIVE BAND PASS		PASSIVE LOW PASS	
ALL ↓	k	1	n	1	n
	N_k	N_1	N_n	N_{1L}	N_{nL}
	R_k	$-R_1$	R_n	R_1	R_n
a	B_k	$\frac{1}{R_1}(Q_d + \Delta Q_1)\eta$	$\frac{1}{R_n}(q_c + \Delta q_n)\eta$	$\frac{1}{R_1}\frac{\omega}{\omega_{01}}$	$\frac{1}{R_n}\frac{\omega}{\omega_{0n}}$
b	X_k	$R_1(Q_d + \Delta Q_1)\eta$	$R_n(q_c + \Delta q_n)\eta$	$R_1\frac{\omega}{\omega_{01}}$	$R_n\frac{\omega}{\omega_{0n}}$
c	B_k	$\frac{1}{R_1}Q_d\eta$	$\frac{1}{R_n}q_c\eta$	$\frac{1}{R_1}\frac{\omega}{\omega_{01}}$	$\frac{1}{R_n}\frac{\omega}{\omega_{0n}}$
	X_k'	$R_1(Q_d' + \Delta Q_2)\eta$	$R_n(q_c' + \Delta q_{n-1})\eta$	$R_1\frac{\omega}{\omega_{01}'}$	$R_n\frac{\omega}{\omega_{0n}'}$
d	X_k	$R_1 Q_d\eta$	$R_n q_c\eta$	$R_1\frac{\omega}{\omega_{01}}$	$R_n\frac{\omega}{\omega_{0n}}$
	B_k'	$\frac{1}{R_1}(Q_d' + \Delta Q_2)\eta$	$\frac{1}{R_n}(q_c' + \Delta q_{n-1})\eta$	$\frac{1}{R_1}\frac{\omega}{\omega_{01}'}$	$\frac{1}{R_n}\frac{\omega}{\omega_{0n}'}$

$\eta = \frac{\omega}{\omega_0} - \frac{\omega_0}{\omega}$

Fig. 6. Pass band reactive constraint networks.

in accordance with the stability and realizability requirements [3] on W_A and on $\rho_1(p)$. Assuming that no degenerate transmission zeros of N_{nL}, N_{0L}, and N_{1L} exist, then there exists a gain integral [28] subject to Re (p_{0i}) and Re $(p_{pi}) < 0$, corresponding to each nonzero low-pass reactive constraint imposed by N_{1L} and N_{nL}. In particular, for normalized inverse inductances or capacitances ω_{01}, ω_{01}', ω_{0n}, ω_{0n}' defined in Fig. 6, the integrals are

$$\int_0^\infty \ln\left(\frac{1}{|\rho_1|}\right) d\omega = \pi\omega_{01} = \frac{\pi}{2}\left[\sum_i (p_{0i} - p_{pi})\right]; \quad (\omega_{01} < \infty) \quad (4a)$$

$$\int_0^\infty \ln\left(\frac{1}{|\rho_n|}\right) d\omega = \pi\left[\omega_{0n} + \sum_i p_{0i}\right]; \quad (\omega_{0n} < \infty) \quad (4b)$$

$$\int_0^\infty \omega^2 \ln\frac{1}{|\rho_1|} d\omega = -\frac{\pi}{3}\omega_{01}^3\left(1 - 3\frac{\omega_{01}'}{\omega_{01}}\right) = -\frac{\pi}{6}\sum_i (p_{0i}^3 - p_{pi}^3); \quad (\omega_{01}, \omega_{01}' < \infty) \quad (4c)$$

$$\int_0^\infty \omega^2 \ln\frac{1}{|\rho_n|} d\omega = -\frac{\pi}{3}\left[\omega_{0n}^3\left(1 - 3\frac{\omega_{0n}'}{\omega_{0n}}\right) + \sum_i p_{0i}^3\right] \quad (\omega_{0n}, \omega_{0n}' < \infty). \quad (4d)$$

For lossless equalization, $|\rho_1| = |\rho_n|$, so that the following relationships between existing reactive constraints, obtained from (4), must be satisfied:[2]

$$\omega_{01} - \omega_{0n} = \sum_i p_{0i}; \qquad (\omega_{01}, \omega_{0n} < \infty) \quad (5a)$$

$$\omega_{01}^3\left(1 - 3\frac{\omega_{01}'}{\omega_{01}}\right) - \omega_{0n}^3\left(1 - 3\frac{\omega_{0n}'}{\omega_{0n}}\right) = \sum_i p_{0i}^3 \quad (\omega_{01}, \omega_{01}', \omega_{0n}, \omega_{0n}' < \infty). \quad (5b)$$

The relationships (4) and (5) may be expressed in terms of the parameters of the active band-pass constraint networks N_n and N_1 representing the pass band circulator and device models by utilizing the low-pass band-pass element equivalence [7] suggested in Fig. 6, as follows:

$$\omega_{01} = \frac{\omega_0}{Q_d + \Delta Q_1} \leq \frac{\omega_0}{Q_d}; \quad \omega_{01}' = \frac{\omega_0}{Q_d'} = \infty \quad (6a)$$

$$\omega_{01} = \frac{\omega_0}{Q_d}; \quad \omega_{01}' = \frac{\omega_0}{Q_d' + \Delta Q_2} \leq \frac{\omega_0}{Q_d'} \quad (6b)$$

$$\omega_{0n} = \frac{\omega_0}{q_c + \Delta q_n} \leq \frac{\omega_0}{q_c}; \quad \omega_{0n}' = \frac{\omega_0}{q_c'} = \infty \quad (6c)$$

$$\omega_{0n} = \frac{\omega_0}{q_c}; \quad \omega_{0n}' = \frac{\omega_0}{q_c' + \Delta q_{n-1}} \leq \frac{\omega_0}{q_c'} \quad (6d)$$

where the terms ΔQ_1, ΔQ_2, Δq_n, Δq_{n-1} absorb any augmentation[1] of the resonators in N_1 and N_n adjacent to N_0 that may be required by the synthesis.

Substitution of (6) in (4a) and (4b) yields the gain integral

[2] In the completely passive case treated by Fielder [28], right half plane zeros of $\rho_1(p)$ are permitted, so that relationships such as (5) may always be satisfied without restrictions on ω_{01}, ω_{01}', ω_{0n}, and ω_{0n}', by adding appropriate right half plane zeros to $\rho_1(p)$ in such a manner as not to alter $|\rho_1(p)|$.

$$\int_0^\infty \ln\left(\frac{1}{|\rho_1|}\right) d\omega = \pi \min\left[\frac{\omega_0}{Q_d}, \frac{\omega_0}{q_c} + \omega_c \sum_i \tilde{p}_{0i}\right]$$

$$= \frac{\pi}{2} \omega_c \sum_i (\tilde{p}_{0i} - \tilde{p}_{pi}) \tag{7}$$

where

$$\tilde{p}_{0i} = \frac{p_{0i}}{\omega_c},$$

$$\tilde{p}_{pi} = \frac{p_{pi}}{\omega_c},$$

ω_c = frequency scaling parameter.

Substituting (6) and (7) in (5) yields a set of "compatibility conditions" on pass band device and circulator selectivities Q_d, Q_d', q_c, and q_c' for which lossless equalization is possible, as presented in Table II. If lossless equalization is possible, it is designated device-limited, circulator-limited, or equally limited, depending upon whether ω_0/Q_d is less than, greater than, or equal to

$$\frac{\omega_0}{q_c} + \omega_c \sum_i \tilde{p}_{0i}.$$

The gain-bandwidth limitations corresponding to these cases are also presented in Table II. They are obtained by solving (7) for ω_c and noting that the fractional bandwidth β of the amplifier, however defined, is of the form

$$\beta = \frac{f^+ - f^-}{f_0} = \frac{\omega_c}{\omega_0} K(W_{AO}, \tilde{p}_{0i}, \tilde{p}_{pi}) \tag{8a}$$

$$f^\pm = \frac{f_0}{2}\left[\sqrt{\beta^2 + 4} \pm \beta\right] \tag{8b}$$

where $W_{AO} = W_A(f_0)$, ω_c, $\tilde{p}_{0i}$ and $\tilde{p}_{pi}$ characterize the arbitrary specified gain function W_A.

Examination of Table II shows that the heretofore unrecognized lossless equalization requirements on q_c/Q_d, q_c', and Q_d', and gain-bandwidth limitations on β presented here, are generally more restrictive than equivalent restrictions obtained in the past [3]–[11] under the perfect circulator assumption ($q_c = q_c' = 0$). In particular, lossless equalization is generally not possible if both q_c' and Q_d' are nonzero, and is sometimes not possible even if one of these is zero. Furthermore, the gain-bandwidth limitations corresponding to circulator-limited equalization can be considerably more restrictive (by a factor of $(Q_d/q_c)\Phi(W_A) < 1$) than those for device-limited equalization.

C. Results for Specified Reflection Gain Characteristics

The general results obtained above may be applied to particular gain functions $W_A(f)$ by substituting the particular values of W_{AO}, $\tilde{p}_{0i}$, $\tilde{p}_{pi}$, and ω_c corresponding to W_A in (4), (5), (7), and (8) and, hence, in Table II. In particular, the requirements for lossless equalization and the corresponding gain-bandwidth limitations for the ideally flat gain characteristic and for the nth-order Butterworth and Chebyscheff approximations [3] of it are presented in Table III. In addition, gain-bandwidth curves for both device- and circulator-limited Butterworth equalization are presented in Fig. 7.

TABLE II

GENERAL REQUIREMENTS FOR LOSSLESS EQUALIZATION AND GAIN-BANDWIDTH LIMITATIONS

Parameter and Bandwidth Limitations	Lossless Equalization Limited by:		
	Device	Circulator	Both
$\frac{q_c}{Q_d}$	$\leq \Phi(W_A)$	$\geq \Phi(W_A)$	$\Phi(W_A)$
Q_d'	$\leq \Psi_d(W_A)$	0	$\leq \Psi_d(W_A)$
q_c'	0	$\leq \Psi_c(W_A)$	$\leq \Psi_c(W_A)$
β	$\frac{2K}{Q_d \sum_{i=1}^{n} (\tilde{p}_{0i} - \tilde{p}_{pi})}$	$\frac{2K}{q_c \left\lvert \sum_{i=1}^{n} (\tilde{p}_{0i} + \tilde{p}_{pi}) \right\rvert}$	$\frac{2K}{Q_d \sum_{i=1}^{n} (\tilde{p}_{0i} - \tilde{p}_{pi})}$

$$\Phi(W_A) = \frac{\sum_{i=1}^{n} (\tilde{p}_{pi} - \tilde{p}_{0i})}{\sum_{i=1}^{n} (\tilde{p}_{pi} + \tilde{p}_{0i})}; \qquad \Psi_d(W_A) = \frac{3Q_d}{1 + \frac{1}{2}(w_c Q_d)^3 \sum_{i=1}^{n} (\tilde{p}_{pi}^3 - \tilde{p}_{0i}^3)}$$

$$\Psi_c(W_A) = \frac{3q_c}{1 + \frac{1}{2}(w_c q_c)^3 \sum_{i=1}^{n} (\tilde{p}_{pi}^3 + \tilde{p}_{0i}^3)}$$

The results presented in Table III and Fig. 7 indicate that, for moderate midband gain ($W_{AO} < 100$), if lossless Butterworth and Chebysheff equalization is possible, it is circulator-limited unless q_c is considerably less than Q_d ($q_c/Q_d < \Phi \lesssim 0.5$). In addition, the fractional bandwidth $q_c\beta$ obtained under circulator-limited equalization is less by the factor Φ than that $Q_d\beta$ obtainable under device-limited equalization. Another interesting result (Fig. 7) is that for circulator-limited Butterworth equalization, the maximum bandwidth at fixed W_{AO} and q_c is obtained at some finite n, rather than at $n = \infty$ as is the case for all device-limited equalization [3] and for circulator-limited Chebyscheff equalization. Finally, lossless ideally flat gain equalization (obtained from the nth-order Butterworth or Chebyscheff approximations in the limit $n \to \infty$, $\epsilon^2 \to 0$), requires a "perfect" circulator for nonzero bandwidth. The resulting familiar device-limited gain-bandwidth relationship [3]–[5], [8], expressed as

$$\beta = \frac{2\pi}{Q_d \ln W_{AO}}, \tag{9}$$

applies only to the "perfect" circulator case and is far beyond the maximum bandwidth capability when band-limited circulators are employed.

An example illustrating the determination of the gain-bandwidth restrictions imposed upon the realization of a third-order Butterworth gain characteristic by a particular circulator and active device is presented in Appendix I.

TABLE III

REQUIREMENTS FOR LOSSLESS EQUALIZATION AND GAIN-BANDWIDTH LIMITATIONS FOR SPECIFIED W_A

Parameter (Table II)	Specified Gain Function W_A		
	Butterworth	Chebyscheff	Ideal
W_A	$W_{A0}\dfrac{1+(\eta/w_c)^{2n}}{1+W_{A0}(\eta/w_c)^{2n}}$	$W_{A0}\dfrac{1+\epsilon^2T_n^2(\eta/w_c)}{1+\epsilon^2W_{A0}T_n^2(\eta/w_c)}$	W_{A0}: $0 \le \lvert\eta\rvert \le w_c$ 1: $\lvert\eta\rvert > w_c$
$\Phi(W_A)$	$\dfrac{1-\lambda}{1+\lambda}$	$\dfrac{x-y}{x+y}$	0
$\Psi_d(W_A)$	$\dfrac{Q_d\Gamma^- \sin\frac{3\pi}{2n}}{\sin\frac{\pi}{2n}}$	$\dfrac{Q_d\Gamma^- \sin\frac{3\pi}{2n}}{\sin\frac{\pi}{2n}}$	$3Q_d$
$\Psi_c(W_A)$	$\dfrac{q_c\Gamma^+ \sin\frac{3\pi}{2n}}{\sin\frac{\pi}{2n}}$	$\dfrac{q_c\Gamma^+ \sin\frac{3\pi}{2n}}{\sin\frac{\pi}{2n}}$	$3q_c$
$\Gamma^{\pm}$	$\dfrac{(W_{A0}^{1/2n}\pm 1)^2}{W_{A0}^{1/n}\pm 2W_{A0}^{1/2n}\cos\frac{\pi}{n}+1}$	$\dfrac{(x\pm y)^2}{x^2+y^2\pm 2xy\cos\frac{\pi}{n}+\sin^2\frac{\pi}{n}}$	—
Device-limited β	$\dfrac{2}{Q_d}\dfrac{\sin\frac{\pi}{2n}}{W_{A0}^{1/2n}-1}\left[\dfrac{1-\alpha}{\alpha-\frac{1}{W_{A0}}}\right]^{1/2n}$	$\dfrac{2}{Q_d}\left[\dfrac{\sin\frac{\pi}{2n}}{x-y}\right]$	$\dfrac{2\pi}{Q_d\ln W_{A0}}$
Circulator-limited β	$\dfrac{2}{q_c}\dfrac{\sin\frac{\pi}{2n}}{W_{A0}^{1/2n}+1}\left[\dfrac{1-\alpha}{\alpha-\frac{1}{W_{A0}}}\right]^{1/2n}$	$\dfrac{2}{q_c}\left[\dfrac{\sin\frac{\pi}{2n}}{x+y}\right]$	0

1) Device (circulator) limited equalization requires $\dfrac{q_c}{Q_d}\le(\ge)\Phi(W_A)$, $Q_d'\le\Psi_d\ (=0)$, and $q_c'=0\ (\le\Psi_c)$.

2) $\beta=w_c\left(\dfrac{1-\alpha}{\alpha W_{A0}-1}\right)^{1/2n}$ for Butterworth W_A and w_c for Chebyscheff and ideal W_A.

3) $x=\sinh\left(\dfrac{1}{n}\sinh^{-1}\dfrac{1}{\epsilon}\right)$; $y=\sinh\left(\dfrac{1}{n}\sinh^{-1}\dfrac{1}{\sqrt{W_{A0}}\,\epsilon}\right)$, $\lambda=W_{A0}^{-1/2n}$.

4) $T_n=n$th-order Chebyscheff polynomial.

5) $r=$pass band ripple$=\dfrac{1+\epsilon^2W_{A0}}{1+\epsilon^2}$.

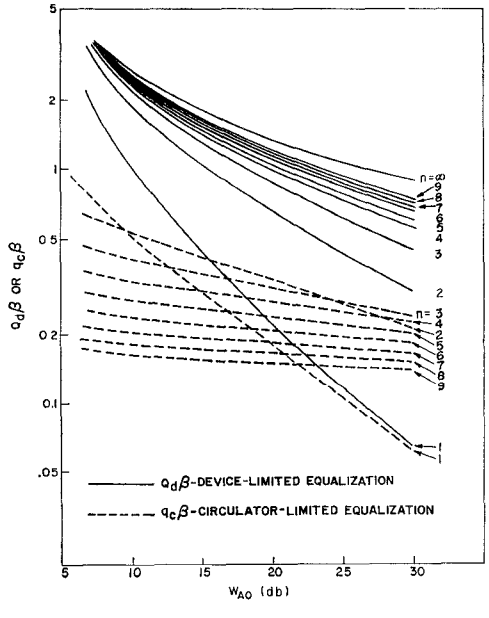

Fig. 7. Half-power bandwidths for device- and circulator-limited Butterworth equalizations.

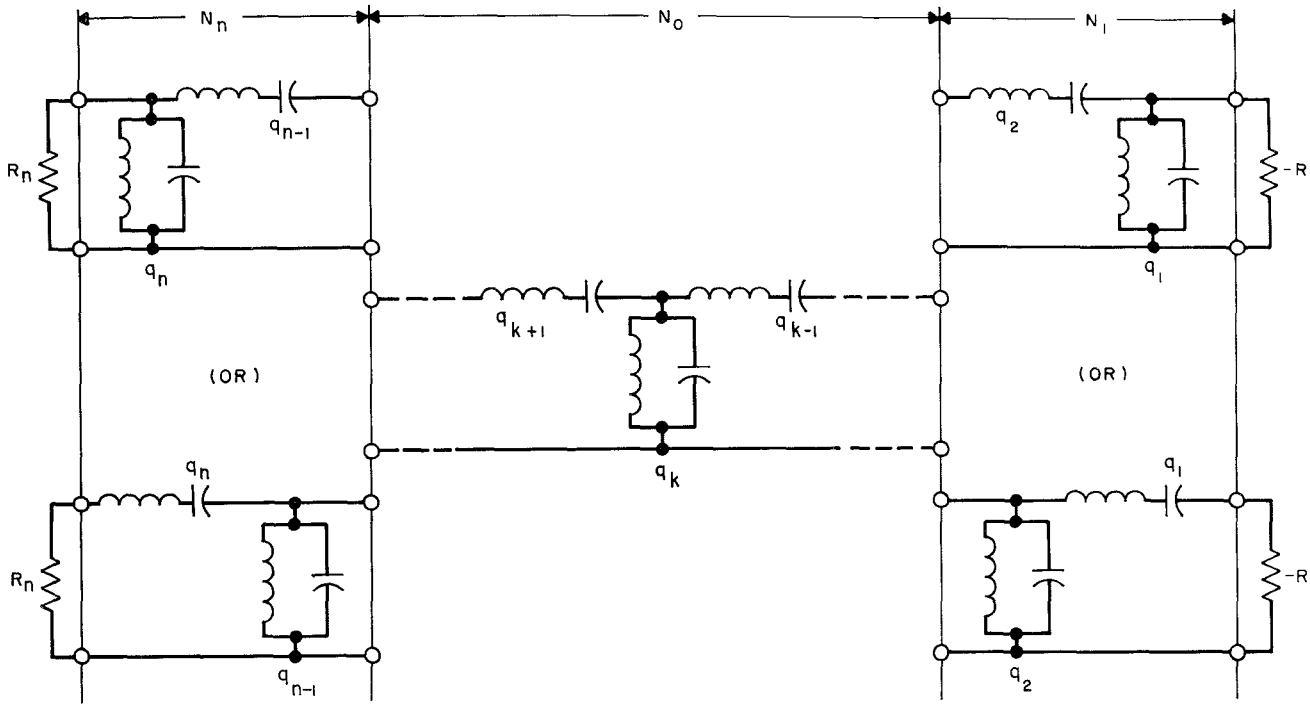

Fig. 8. Pass band prototype equalization ladder network.

D. Synthesis of Pass Band Equalization Network

The nth-order Butterworth and Chebyscheff reflection gain functions discussed in the preceding section may be realized, assuming lossless equalization is possible, by synthesizing N (Fig. 1) such that, in the amplifier pass band, it is representable by a lossless band-pass ladder network, which includes the reactive constraints of the pass band transformed circulator and active device models. The resulting pass band prototype of N is a cascade of $N_n+N_0+N_1$, containing n alternate shunt and series band-pass resonators tuned to f_0 as shown in Fig. 8.

The selectivities $q_1, q_2, \cdots, q_n$ of the n band-pass resonators, normalized to R_n as defined in Fig. 8, may be calculated from existing formulas for the normalized element values $\gamma_1, \gamma_2, \cdots, \gamma_n$, derived [29], [30] for the passive low-pass prototypes corresponding to both Butterworth and Chebyscheff equalization. In particular,

$$q_l = \begin{cases} \dfrac{\gamma_l}{w_c}\dfrac{R_1}{R_n} & \text{for series resonators} \\ \dfrac{\gamma_l}{w_c}\dfrac{R_n}{R_1} & \text{for shunt resonators} \end{cases} \tag{10}$$

where

$l=1, 2, \cdots, n,$
$w_c=\omega_c/\omega_0.$

An example of the design of a pass band equalization network for a specified gain characteristic and a given circulator and active device is provided in Appendix I.

For cases where the pass band device and circulator models do not satisfy the lossless equalization requirements for given W_A (Tables II and III), particular reactive elements may be added at the transformed circulator and/or device terminals, so as to yield new pass band models which crudely approximate those of Fig. 6 with new selectivities that satisfy the lossless equalization requirements. An alternative approach is to realize N as a cascade of a lossless band-pass ladder N_d and a constant resistance band pass band reject filter pair N_c [6]. If N_c and N_d absorb the constraining networks N_n and N_1 representing the circulator and device respectively, they may be synthesized to yield a $W_A(f) \approx W_d(f)u(f)$, where $W_d>1$ is constrained only by the device, and $u\leq 1$ only by the circulator, thereby eliminating the compatibility problem. Each of these approaches, however, usually results in a relatively crude approximation of the desired gain characteristic and introduces additional bandwidth limitations not attributable to the device or circulator alone.

IV. Stabilization and Overall Synthesis

A. Determination of Stability Bandwidth

The pass band equalization described above guarantees amplifier stability only over the frequency range

about f_0 for which the pass band models of the device, circulator, and equalizing network are valid. To prevent oscillation at other frequencies in the active range $(\Delta\omega)_A$ of the device, due to the out-of-band immittance behavior of the circulator and device, additional stabilizing circuitry is required. The first step in the stabilization is the determination, using appropriate stability criteria at any reference plane in N_T, of ω_H and ω_L, the closest frequencies in $(\Delta\omega)_A$ to ω_0 of potential instability under the *exact* circulator, device, and matching network representations. (If no ω_H and ω_L exist in $(\Delta\omega)_A$, no further stabilization is required.) The stability bandwidth β_s, defined as

$$\beta_s = \frac{\omega_s^+ - \omega_s^-}{\omega_0}; \qquad \omega_s^+\omega_s^- = \omega_0^2$$

$$\omega_s^+ = \min\left(\omega_H, \frac{\omega_0^2}{\omega_L}\right); \quad \omega_s^- = \max\left(\omega_L, \frac{\omega_0^2}{\omega_H}\right), \tag{11}$$

is then used to synthesize the appropriate stabilizing circuitry.

The most applicable stability criterion is the complex plane criterion on the total immittance $H(p)$ [total node admittance $Y(p)$ or loop impedance $Z(p)$] at the active device terminals. This follows from the basic stability condition that $H(p)$ have no zeros in complex frequency $p=\sigma+j\omega$ such that Re $(p)\geq 0$. Applying the Nyquist criterion to $H(p)$, the complex plane criterion [25] is stated as follows.[3]

A necessary and sufficient condition for stability is that n_c, the net number of counterclockwise encirclements of the origin of the complex immittance plane (H-plane) made by the locus of $H(j\omega)$ as $-\infty \leq \omega \leq +\infty$, be equal to P, the number of poles of $H(p)$ having Re $(p)>0$, or[3]

$$n_c = P. \tag{12}$$

A proposed real immittance function stability criterion derived from the above, which only requires separate examination of the real and imaginary parts of $H(j\omega)$ over $(\Delta\omega)_A$, is presented in Appendix II. In addition, a useful reflection coefficient stability criterion is presented by Henoch and Kvaerna [6].

Correct application of any of the above stability criteria requires that $H_d(j\omega)$, and $H_N(j\omega)$, the components of $H(j\omega)=H_d(j\omega)+H_N(j\omega)$ representing the active device terminal immittance and that of the passive circuitry facing it, respectively, be known accurately over all $(\Delta\omega)_A$ rather than be based on pass band models. Then, for the types of devices under consideration, it is shown in Appendix II that a stability study usually yields the following simple condition on $H(j\omega)=U(\omega)+jV(\omega)$ for determining ω_L and ω_H:

$$\omega_L = \omega_{\max} < \omega_0 \quad \text{and} \quad \omega_H = \omega_{\min} > \omega_0$$

such that

$$U(\omega) < 0, \qquad V(\omega) = 0. \tag{13}$$

Application of (13) to (11) yields the nominal stability bandwidth for H_N, representing the given circulator and the equalizing network for the specified W_A, and for H_d the given device at its nominal operating point with respect to energizing (bias or pump) voltage. Repetition of this process for the range of functions H_d, corresponding to the expected range of energizing voltages to which the device may be subjected, yields a series of ω_H, ω_L pairs from which a lower bound β_{s0} on β_s may be obtained. β_{s0} is then the bandwidth for absolute amplifier stability which, while not essential, is desirable in practice since conditionally stable amplifiers could experience unquenchable oscillation due to large signals or transient bias shifts.

B. Stabilization of Amplifier

Potential amplifier instability outside of β_s (or β_{s0}) is eliminated by the incorporation in network N (Fig. 1) of a stabilizing network N_S which introduces sufficient out-of-band ohmic loss to effectively "passivate" the active device outside β_s while appearing essentially reactive in the amplifier pass band. It has been shown [6] that the configuration for N_S, which provides most efficient out-of-band stabilization with the least pass band gain perturbation, is a one-port resistively terminated band rejection ladder network (Fig. 9), series or shunt connected at the active device terminals. The desired pass band gain equalization is maintained by absorbing the reactive pass band input immittance of N_S, that of a single resonator tuned to ω_0, in the pass band equalizer as shown in Fig. 10. For optimum stabilization, N_S should be connected as close as possible to the negative resistance of the active device, consistent with stability requirements and with the resonator selectivity requirements for pass band equalization.

The stability requirement on N_S in terms of the real part U_{st} of its input immittance $H_{st}=U_{st}+jV_{st}$ ($H_{st}=Z_{st}$ or Y_{st} for series- or shunt-connected N_S, respectively) is obtained from (13) or Appendix II, under the restriction[4] that N_S be connected no further away from the active device than in series or shunt with the second resonator of $N_1(k=2$, Fig. 10). The requirement on $U_{st}(\omega)$ in terms of device terminal immittance $H_d(j\omega)$ and stabilizing network termination U_{0s} is

$$|\, U_d(\omega)\,|_{\max} = U_{st}(\omega_s^{\pm}) = a_s U_{0s} < U_{st}(\omega) \leq U_{0s} \tag{14}$$

for all ω outside the interval (ω_s^-, ω_s^+).

[3] This assumes $H(p)$ has no essential singularities in p with $\mathrm{Re}(p)\geq 0$, particularly at infinity, and that the active frequency range $(\Delta\omega)_A$ of the negative resistance device is finite. Both assumptions are valid for physical devices and network elements. In addition, all poles of $H(p)$ with $\mathrm{Re}(p)>0$ are contributed by $H_d(p)$, the component due to the active device. For poles of $H(p)$ at $p=j\omega_R$, $H(j\omega)$ near ω_R is evaluated by replacing $j\omega_R$ by $j\omega_R+re^{j\phi}$ with $r\to 0$, $-(\pi/2)\leq\phi\leq(\pi/2)$.

[4] Otherwise, the band rejection stabilizing network under consideration cannot present an input immittance characteristic which satisfies the relevant stability criterion for the large number P of RHP poles of $H(p)$ at the reference plane of N_S.

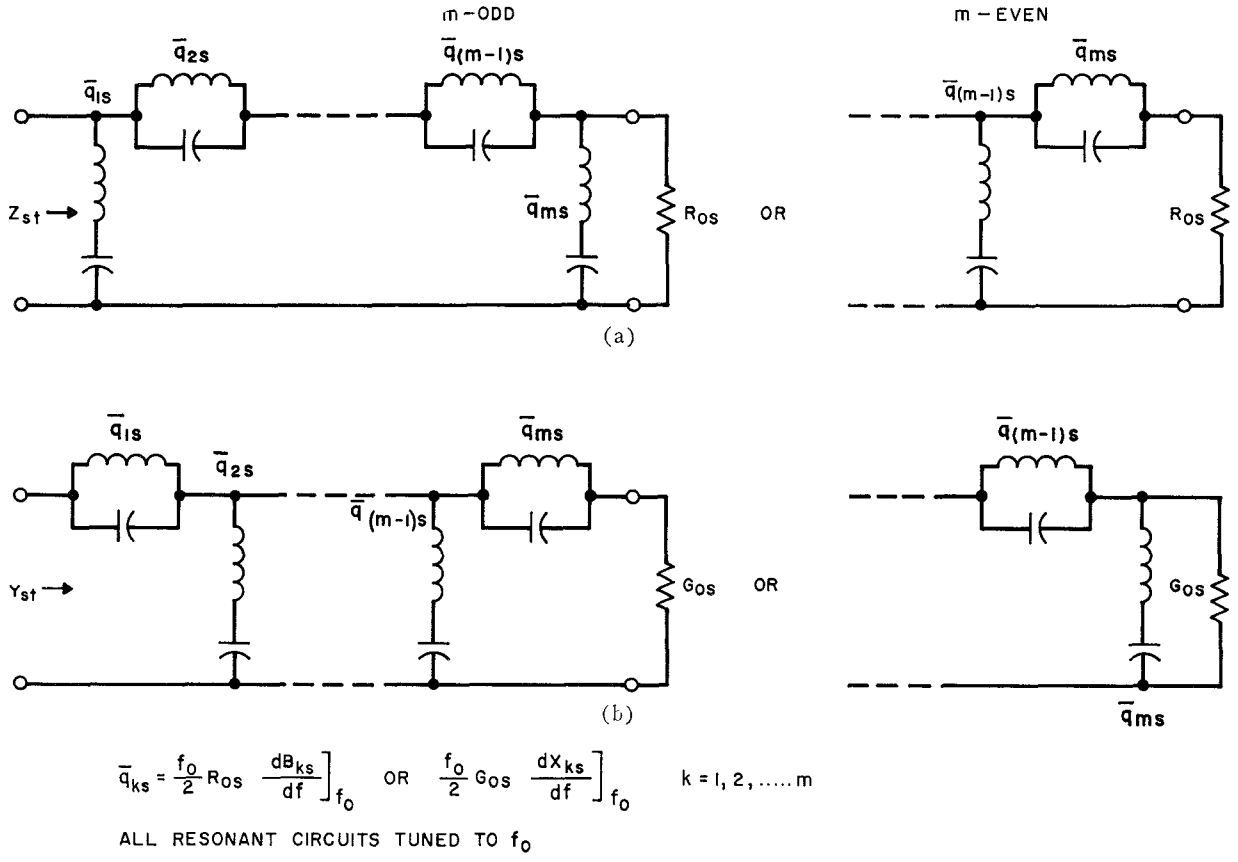

Fig. 9. Pass band prototype ladder representation of stabilizing network. (a) Series-connected N_S. (b) Shunt-connected N_S.

The desired behavior of H_{st} is obtained if N_s is synthesized to realize an mth-order Butterworth approximation of ideal band rejection behavior in U_{st}, as given by

$$U_{st} = \frac{U_{0s}(\eta/w)^{2m}}{1+(\eta/w)^{2m}}; \qquad \eta = \frac{\omega}{\omega_0} - \frac{\omega_0}{\omega} \tag{15}$$

where w and U_{0s} are obtained, for a given $U_d(\omega)$ and an arbitrary choice of a_s, by substituting (14) in (15).

In the amplifier pass band, input immittance H_{st} becomes essentially purely reactive, given by

$$H_{st} \approx jV_{st} \approx jU_{0s}\bar{q}_{st}\eta. \tag{16}$$

For Butterworth U_{st}, $\bar{q}_{st}$ is simply

$$\bar{q}_{st} = \bar{q}_{1s} = \frac{1}{wm \sin\frac{\pi}{2m}}. \tag{17}$$

The selectivities q_{js} of the resonators comprising N_S, as defined in Fig. 9, may be obtained from the normalized Butterworth low-pass elements γ_j $(j=1, 2, \cdots, m)$ used in the pass band equalization (10), employing

$$\bar{q}_{js} = \frac{1}{w\gamma_j}\Bigg]_{R_1=0}; \qquad j = 1, 2, \cdots, m \tag{18}$$

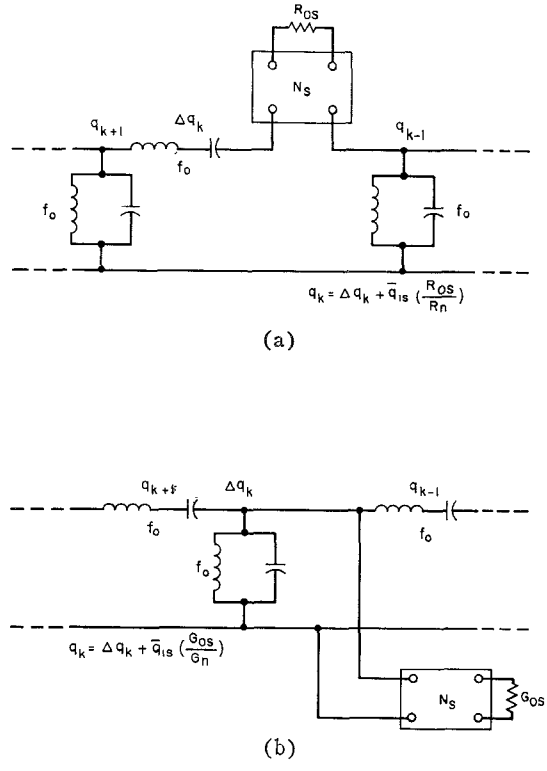

Fig. 10. Absorption of stabilizing network in pass band equalizer. (a) Series-connected N_S. (b) Shunt-connected N_S.

where the limit on γ_j as $R_1 \to 0$ is taken such that

$$1 - W_{A0}^{-1/2n} \to \frac{2}{n}\frac{R_1}{R_n}.$$

An example of the stabilization of a particular amplifier is presented in Appendix I.

The overall synthesis of coupling network N involves the interconnection of stabilizing network N_S and pass band equalizer N_0 such that the pass band H_{st} due to N_S is absorbed in the first or second resonator (q_1 or q_2) of N_1 (Fig. 8) as shown in Fig. 10. Whether H_{st} is absorbed in q_1 or q_2 depends upon which choice allows the given $\bar{q}_{st}$, Q_d, Q_d', q_c, and q_c' to be included in the total selectivities q_1, q_2, q_{n-1}, and q_n determined for the given W_A using Tables II and III, and (10) with the most stability margin and the least, if any, degradation in bandwidth. The remaining resonator selectivities required for the synthesis of N are obtainable from [29], [30], (6), (10), and (18). The various resonators comprising N_0 and N_S may be realized [31] in various microwave transmission media, preferably as combinations of semilumped transmission line elements, having first higher order resonances well above f_0.

V. Experimental Verification of Theory

A. Amplifier Design Procedure

In order to verify the theory of the preceding sections, an L-band coaxial tunnel diode amplifier having the configuration of Fig. 1 was designed, constructed, and tested, using a three-port strip-junction circulator with 50 ohm coaxial output ports and a 30 ohm germanium tunnel diode. The difference in circulator and diode impedance level required the use of a quarter-wave impedance transformer N_X (Fig. 1) for stable high-gain amplification.

The complete design procedure for network N is outlined in Appendix I under the boundary conditions imposed by the measured diode and transformed circulator equivalent circuits, as shown in Fig. 11(b). The amplifier center frequency, as set by the circulator, is $f_0 = 1.46$ Gc/s. Specification of a third-order Butterworth gain characteristic results in a strongly circulator-limited bandwidth capability (Appendix I). This permits the connection of a shunt-connected stabilizing network at the tunnel diode terminals [Fig. 11(b)] with Y_{st} absorbed in the first resonator, without degrading the amplifier bandwidth capability. Network element values are obtained in Appendix I using (10) and (18) for two separate equalizer designs (I and II) corresponding to $W_{A0} = 10$ and 40, respectively.

The fairly conventional coaxial physical realization of coupling network N_T has the equivalent circuit of Fig. 11(a), which reduces to the three-section pass band prototype model implicit in Fig. 11(b). The design utilizes resonators which are adjustable in q and f_0 and

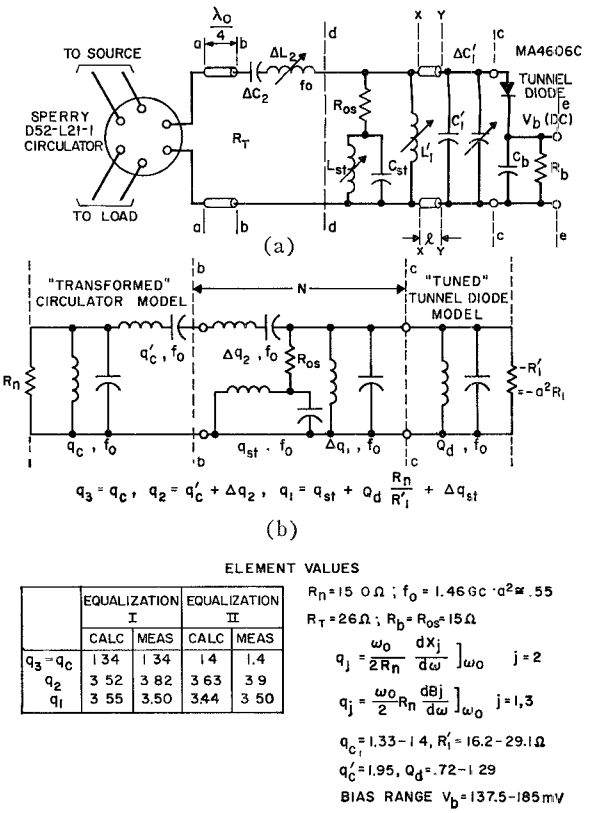

Fig. 11. (a) Equivalent circuit of overall coupling network N_T for experimental tunnel diode amplifier. (b) Pass band prototype of coupling network N, including circulator and diode constraints.

which have been individually precalibrated over their entire range of adjustment in the amplifier structure. This permits pretuning to nominal calculated values and final adjustment for the desired measured gain characteristics. A comparison of nominal and final adjustment values of the pass band prototype resonator selectivities is presented in Fig. 11(b) for designs I and II. The resonator precalibrations and the circulator and diode characterizations are all based on RF immittance measurements in suitable modifications of the amplifier structure and, hence, include the effect of all structural discontinuities.[5]

B. Measured Performance Versus Theory

The measured, absolutely stable, maximally flat reflection gain characteristics $W_A(f)$ corresponding to equalizer designs I and II are compared with their

[5] The structure of Fig. 11(a) was designed so that the sections between reference planes $a-a$ and $d-d$, $d-d$ and $c-c$, and $c-c$ and $e-e$ could be separated, with each terminated at either end in 50-ohm coaxial connectors. This permitted individual RF immittance measurements (over a range of resonator settings when appropriate) of the mounted diode, the "transformed" circulator (through ΔL_2, ΔC_2), resonator ΔL_2, ΔC_2, resonator L_1', C_1', $\Delta C_1'$, and the stabilizing network R_{0s}, L_{st}, C_{st} in the same geometry as in the assembled N_T, thereby including the effects of discontinuities. Similar short-circuit admittance measurements on N_T yielded the values of series and shunt loss resistances R_{Ls} and G_{LP}.

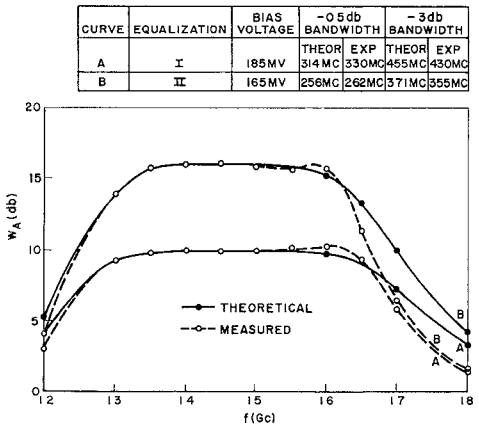

Fig. 12. Measured and calculated maximally flat reflection gain $W_A(f)$ of experimental tunnel diode amplifier.

theoretical counterparts in Fig. 12, including a tabular comparison of -0.5 dB and -3 dB bandwidths. The agreement in bandwidth with theory is within 6 percent, and the residual pass band ripple in the nominally flat measured $W_A(f)$ is less than 0.5 dB. This compares with ripple possibly as high as 2.75 dB and 5.70 dB which might be obtained [eq. (2)] at 10 dB and 16 dB gain, respectively, for the given circulator ($|s'| \lesssim 0.05$) under a "perfect" circulator synthesis. Finally, the experimental amplifier was found to be absolutely stable over all diode bias and input and output terminations for both designs I and II.

VI. Summary and Conclusions

Gain-bandwidth limitations, derived for a circulator-coupled, negative resistance reflection amplifier, under restrictions imposed by proposed frequency-dependent circuit models for circulators and broadband negative resistance devices, are considerably more restrictive than past results which only considered some of the limitations of the latter. In particular, the inherent selectivity of the ferrite junction of the circulator is frequently the bandwidth limiting element. Furthermore, an overall synthesis procedure, presented for realization of an absolutely stable amplifier having a specified band-pass power gain characteristic, includes a stabilization network to suppress out-of-band oscillations. Finally, the theory has been verified by the construction and testing of an L-band tunnel diode amplifier, which exhibited third-order maximally flat gain, centered at 1.46 Gc/s and with half-power bandwidth within 6 percent of the calculated values.

Appendix I
Design Example: L-Band Tunnel Diode Amplifier

A. Circulator and Device Characteristics

The circulator-coupled tunnel diode reflection amplifier to be designed has the general configuration shown in Fig. 1. The circulator is a Sperry D-52-L21-1 #1 stripline wye-junction type with three coaxial output ports at nominal impedance level $R_0 = 50$ ohms. The circulator pass band, 1.2–1.8 Gc/s, is centered at $f_0 = 1.46$ Gc/s. The measured pass band immittance model at the negative resistance port is that of Fig. 2(a)-(2), with $\bar{q}_c = 1.4$ and $\bar{q}_c' = 1.0$.

The tunnel diode is a germanium, Microwave Associates MA4606C #184 in a pill package. Its measured small signal equivalent circuit parameters (Fig. 4) over the useful range of active bias voltage (137.5–185 mV) are $R = 32.9$–52.4 ohms ($R_{\min} = 32.9$ ohm over all bias), $C = 1.9$–2.0 pF, $R_s = 3.0$ ohms, $L = 0.29$ nH, and $C_p = 0.37$ pF. Employing shunt tuning and noting that $k \lesssim 1.5$, the "tuned" tunnel diode model in the circulator pass band is that of Fig. 3(a). Element values for Fig. 3(a) are calculated in terms of the diode parameters over $V_b = 137.5$–185 mV as follows:

$$R_1' = a^2 R_1 \cong a^2 \left[\frac{1 - \alpha_0^2}{R(1 - \delta')(1 - k'\alpha_0^2)^2} - G_{LP} \right]^{-1}$$

$$= 16.2\text{–}29.1 \text{ ohms}$$

$$Q_d = 2\pi f_0 R_1 \left[\frac{C}{(1 - \delta')(1 - k'\alpha_0^2)} + C_p \right] = 0.72\text{–}1.29$$

where $\delta' = (R_s + R_{Ls})/R$; $k' = L/RC(R_s + R_{Ls})$, $\alpha_0 = 2\pi f_0 RC[(1/\delta') - 1]^{-1/2}$, $G_{LP} = 0.0033$ mhos, and $R_{Ls} = 1$ ohm are the measured[5] shunt- and series-circuit loss components referred to the diode terminals, and $a^2 = 0.55$ represents an impedance level transformation[6] at the tuning element. The required tuning inductor is $L_d = R_1'/2\pi f_0 Q_d = 2.46$ nH.

B. Specified Gain Characteristics and Resulting Constraints on Pass Band Equalization

For stable high-gain amplification, we choose N_x (Fig. 1) to be a quarter-wave (at f_0) TEM line transformer of $R_T = 26$ ohms to reduce the circulator impedance level to $R_n = 15$ ohms $< R_1'$ (min), yielding the pass band transformed circulator model of Fig. 2(b)-(1). Comparing pass band circulator and diode models [Figs. 2(b)-(1) and 3(a)], a specified nth-order gain characteristic must have $n = 3, 5, 7 \cdots$. Hence, we specify two separate designs I and II, having third-order Butterworth W_A (Table III, $n = 3$) centered at 1.46 Gc/s and having $W_{AOI} = 10$ and $W_{AOII} = 40$, respectively.

Since $R_1' = R_n(\sqrt{W_{AO}} + 1)/(\sqrt{W_{AO}} - 1)$, the specified midband gains require $R_{II}' = 29.1$ and $R_{III}' = 20.6$ ohms, which are obtained for the given diode at $V_b = 185$ and 165 mV, respectively. The selectivities constraining I and II are $Q_{dI} = 1.29$, $Q_{dII} = 0.91$, $q_{cI} = 1.34$, $q_{cII} = 1.4$, and $q_{cI}' = q_{cII}' = 1.95$.

[6] Immittance measurements on the section between d–d and c–c [Fig. 11(a)] indicate that the unavoidable short transmission line length l between L_1' and C_1' introduces, in the amplifier pass band, an approximately constant step down admittance level transformation $a^2 = 0.55$ between reference planes x–x and y–y, as expected from a leftward looking admittance $Y_L + (1/j\omega L_1')$ at x–x [Fig. 11(a)] having $(\omega |Y_L| L_1')^2 \lesssim 0.1 \ll 1$, rotated through $\beta l \sim 0.1 \ll \pi$ to y–y.

C. Bandwidth Limitations and Prototype Element Values

The first step in the synthesis is the pass band equalizer design. Using the third-order pass band model of Fig. 11(b), the bandwidth limitations are obtained from Table III as follows. For $\Phi(W_A)=(1-\lambda)/(1+\lambda)$ and $\lambda=W_{AO}^{-1/(2n)}$, Table III yields $\Phi_{\mathrm{I}}=0.19$ and $\Phi_{\mathrm{II}}=0.297$ for the given W_{AO} and n. Since $q_{c\mathrm{I}}/Q_{d\mathrm{I}}=1.04\gg\Phi_{\mathrm{I}}$, and $q_{c\mathrm{II}}/Qd_{\mathrm{II}}=1.54\gg\Phi_{\mathrm{II}}$, the equalization I and II are both strongly circulator-limited in bandwidth capability. The resulting fractional bandwidths $(\Delta f)_\alpha$ (Table III) are $(\Delta f)_{\mathrm{I}}=455$ Mc/s and $(\Delta f)_{\mathrm{II}}=371$ Mc/s for $\alpha=0.5$ and $(\Delta f)_{\mathrm{I}}=314$ Mc/s and $(\Delta f)_{\mathrm{II}}=256$ Mc/s for $\alpha=0.891$ (-0.5 dB), respectively. (The comparable figures if $q_c=q_c'=0$, and Q_d were the only constraint, would be $(\Delta f)_{\mathrm{I}}=2.06$ Gc/s and $(\Delta f)_{\mathrm{II}}=1.71$ Gc/s for $\alpha=0.5$ and $(\Delta f)_{\mathrm{I}}=906$ Mc/s, $(\Delta f)_{\mathrm{II}}=755$ Mc/s for $\alpha=0.891$, a tremendous difference.)

To synthesize N_0 (Fig. 8), the normalized low-pass element values, obtained from Weinberg and Slepian [29], for $n=3$ are $\gamma_{1\mathrm{I}}=3.13$, $\gamma_{2\mathrm{I}}=0.812$, $\gamma_{3\mathrm{I}}=1.145$, and $\gamma_{1\mathrm{II}}=2.18$, $\gamma_{2\mathrm{II}}=1.22$, $\gamma_{3\mathrm{II}}=0.89$. The corresponding prototype resonator selectivities, $q_{1\mathrm{I}}=3.55$, $q_{2\mathrm{I}}=3.52$, $q_{3\mathrm{I}}=q_{c\mathrm{I}}=1.34$ and $q_{1\mathrm{II}}=3.44$, $q_{2\mathrm{II}}=3.63$ and $q_{3\mathrm{II}}=q_{c\mathrm{II}}=1.4$ are obtained from (10) using $w_{c\mathrm{I}}=0.445$ and $w_{c\mathrm{II}}=0.463$ as calculated from

$$w_c=\frac{2}{q_c}\left(\frac{\sin\frac{\pi}{2n}}{1+\lambda}\right).$$

D. Stabilization and Overall Synthesis

We apply the real immittance stability criterion (Appendix II) to the exact terminal admittances of the given "tuned" tunnel diode and the passive load terminating it, the circulator seen through N_x and N_0. In the worst case ($V_b=137.5$ mV, $R=R_{\min}=32.9$ ohms) potential instability ($G<0$, $B\approx 0$) is found to exist for frequencies above 3.5 Gc/s. Hence, $f_H=3.5$ Gc/s, $f_L=0$ and, from (11), the stability bandwidth for absolute stability is 2.9 Gc/s ($\beta_{s0}=1.98$). Since $q_1\gg Q_d$ we may connect a single-tuned stabilizing network [Fig. 11(b)] directly across the diode without degrading β. Therefore, choosing $R_{0s}=15$ ohms and $a_s=1.4$ to satisfy (14) for $R_{1\min}'$ and hence for all V_b, we solve (15) for w with $m=1$, $U_{0s}/U_{st}=a_s$, and $\eta=\beta_{s0}$, and substitute the result in (17) yielding $\bar{q}_{1s}=q_{st}=0.8$.

The overall synthesis of N [Fig. 11(b)] is accomplished by absorbing q_c, q_c', Q_d, and q_{st} in q_1, q_2, and q_3 according to the breakdown $q_3=q_c$, $q_2=q_c'+\Delta q_2$, and

$$q_1=Q_d\frac{R_n}{R_1'}+q_{st}+\Delta q_1.$$

Hence, from known values of these parameters, we obtain $\Delta q_{2\mathrm{I}}=1.57$, $\Delta q_{1\mathrm{II}}=2.09$, $\Delta q_{2\mathrm{II}}=1.68$, and $\Delta q_{1\mathrm{III}}=1.98$. The synthesis of N is completed by obtaining the individual L's and C's from

$$C=\frac{1}{\omega_0^2 L}=\frac{q}{\omega_0 R_n}$$

for Δq_2, and

$$L=\frac{1}{\omega_0^2 C}=\frac{qR_n}{\omega_0}\qquad\text{for }\Delta q_1.$$

Appendix II

Real Immittance Function Stability Criterion For Two-Terminal Negative Resistance Devices

The complex plane stability criterion (12) on the total immittance $H(j\omega)=U(\omega)+jV(\omega)$ at the terminals of a one-port negative resistance device may be extended to yield a stability criterion in terms of real functions $U(\omega)$ and $V(\omega)$ as follows.

Let $H(j\omega)=H_d(j\omega)+H_N(j\omega)$ where H_d and H_N are the separate contributions due to the active device and passive terminating network. Hence, $U=U_d+U_N$ and $V=V_d+V_N$. For the active device, $U_d(\omega)\leq 0$ for ω in the active frequency range $\Delta\omega_A=\omega_A^+-\omega_A^-$, so that $U(\omega)$ can be negative within this range. Let $H(j\omega)$ have resonances $V(\omega)=0$ at a discrete set of frequencies ω_1, ω_2, ω_3, $\cdots$ such that $0=\omega_1<\omega_2<\omega_3\cdots$. These resonances may be classified as follows:

1) An "active" resonance[7] ω_j is one at which $U(\omega_j)<0$: $(j=1, 2, \cdots)$.
2) A "singly isolated" active resonance ω_j is one for which $U(\omega_j)$ and either $U(\omega_{j-1})$ or $U(\omega_{j+1})$, but not both, are <0 whereas, for a "doubly isolated" active resonance[7] ω_j, both $U(\omega_{j-1})$ and $U(\omega_{j+1})>0$.
3) A "nonisolated" active resonance ω_j has $U(\omega_{j-1})$, $U(\omega_j)$, and $U(\omega_{j+1})$ all <0.

Then, for a given $H(j\omega)$ we enumerate the various isolated active resonances as follows:

1) Let $n_1^+(n_1^-)$ be the number of singly isolated active resonances ω_j such that

$$\frac{dV}{d\omega}>0\left(\frac{dV}{d\omega}<0\right)$$

at $\omega=\omega_j$.

2) Let $n_2^+(n_2^-)$ be the number of doubly isolated active resonances ω_j such that

$$\frac{dV}{d\omega}>0\left(\frac{dV}{d\omega}<0\right)$$

at $\omega=\omega_j$.

A real imittance function stability criterion may be derived from complex plane criterion (12) as follows. Every possible encirclement of the H-plane origin made

[7] A resonance ω_j at which $U(\omega_j)=0$ corresponds to an imaginary zero of $H(p)$, i.e., $H(j\omega_j)=0$, which represents either a short- or open-circuit at $\omega=\omega_j$ and which is not allowed for stability. Since the existence of such resonances is recognizable without the use of stability criteria, it is assumed that precautions have been taken so that they do not occur. An active resonance at $\omega_1=0$ can be nonisolated or singly isolated but not doubly isolated.

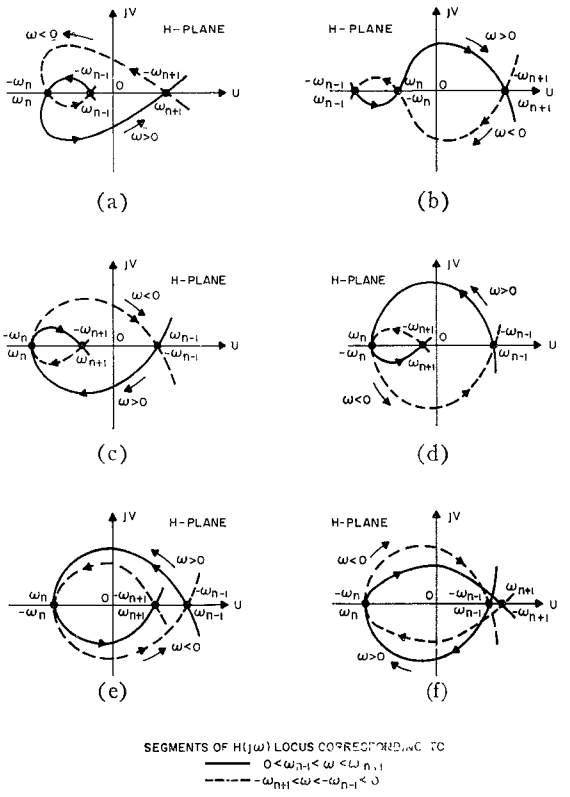

Fig. 13. Possible encirclements of H-plane origin made by $H(j\omega)$ subloci.

TABLE IV

CORRESPONDENCE BETWEEN COMPLEX PLANE ORIGIN ENCIRCLEMENTS AND ISOLATED ACTIVE RESONANCES OF $H(j\omega)$

Figure	Type of active resonance at $\omega=\omega_n$	$\left.\frac{dV}{d\omega}\right\rfloor_{\omega=\omega_n}$	Δn
13(a)	singly isolated	<0	1
13(b)	singly isolated	>0	-1
13(c)	singly isolated	>0	-1
13(d)	singly isolated	<0	1
13(e)	doubly isolated	<0	2
13(f)	doubly isolated	>0	-2

Δn = number of counterclockwise encirclements of origin of H-plane made by subloci of $H(j\omega)$ in Figs. 13 (a)–(f) (k clockwise encirclements $=-k$ counterclockwise encirclements).

by $H(j\omega)$ derives from one of six possible subloci of $H(j\omega)$ corresponding to $0<\omega_{n-1}\leq\omega\leq\omega_{n+1}$, and $-\omega_{n+1}\leq\omega\leq\omega_{n-1}<0$ [the latter since $H(-j\omega)=H^*(j\omega)$] as shown in Fig. 13 (a)–(f). Referring to Fig. 13, a correspondence exists in each case, as summarized in Table IV, between the number of counterclockwise encirclements of the H-plane origin by the $H(j\omega)$ sublocus and the type of isolated active resonance, as described above, which ω_n represents. Based upon this correspondence, the total number n of counterclockwise encirclements by $H(j\omega)(-\infty\leq\omega\leq\infty)$ may be related to the above defined $n_1^{\pm}$, $n_2^{\pm}$. Hence, from (12), a necessary and sufficient condition for stability is

$$n_1^- + 2n_2^- - n_1^+ - 2n_2^+ = P \tag{19}$$

where P is the number of poles of $H(p)$ having Re $(p)>0$.

A sufficient, though not necessary, condition for stabilization which minimizes $n_T=n_1^-+n_1^++n_2^-+n_2^+$ and will henceforth be designated the "optimum sufficiency condition" for stability, is

$$n_1^- + 2n_2^- = P; \qquad n_1^+ = n_2^+ = 0. \tag{20}$$

For the devices represented in Fig. 3, $P=2l$ ($l=0$, 1, or 2), so that the "optimum sufficiency" criterion (20) is satisfied by the choice $n_2^-=l$, $n_1^-=n_1^+=n_2^+=0$. It may be expressed then directly in terms of $U(\omega)$ and $V(\omega)$ as follows:

$U(\omega)>0$ at all $\omega\neq\omega_0$ at which $V(\omega)=0$ except in $l-l_0\geq 0$ isolated narrow frequency bands $(\omega_{aj}, \omega_{bj})$ $(j=1, 2, \cdots, l-l_0)$ which are well removed from the amplifier pass band, with $l_0=0$ for $U(\omega_0)>0$ and $l_0=1$ for $U(\omega_0)<0$. (21a)

$U(\omega)<0$ for ω in $(\omega_{aj}, \omega_{bj})$. (21b)

$V(\omega)=0$ at one and only one $\omega=\bar{\omega}_j$ in $(\omega_{aj}, \omega_{bj})$. (21c)

$dV/d\omega<0$ at $\omega=\bar{\omega}_j$. (21d)

At least one "passive resonance" $[V(\omega)=0, U(\omega)>0]$ exists between each pair of adjacent active frequency bands $[U(\omega)<0]$ of $U(\omega)$. (21e)

For a limited range of device equivalent circuit parameter values, there exist $(l-l_0)$ isolated frequency bands $(\omega_{aj}, \omega_{bj})$ over which $|U_d(\omega)|$ and $-(dV_d/d\omega)$ both $\gg 0$, so that (21b)–(21e) are satisfied automatically for most $H_N(j\omega)$. Therefore, in most cases of interest, the optimum sufficiency condition reduces to

$$U(\omega)>0 \text{ at all } \omega\neq\omega_0 \text{ at which } V(\omega)=0. \tag{22}$$

Alternatively, frequencies of potential instability are those at which $U(\omega)<0$ and $V(\omega)=0$ $(\omega\neq\omega_0)$.

In order to apply the above criteria, we plot $U_N(\omega)$ and $-U_d(\omega)$ vs. ω, and $V_N(\omega)$ and $-V_d(\omega)$ vs. ω over (ω_A^-, ω_A^+) on separate sets of axes, making use of $H=H_d+H_N$.

ACKNOWLEDGMENT

The author would like to express his gratitude to his research advisor, Prof. O. Wing of Columbia University, New York, for his invaluable guidance and encouragement. He also gratefully acknowledges the many useful discussions with Prof. H. E. Meadows, Jr., and Prof. J. Millman of Columbia University, and W. W. Mumford of Bell Telephone Laboratories, Murray Hill, N. J. Finally, he wishes to thank L. D. Gardner of Bell Telephone Laboratories for his assistance in expediting the fabrication of the experimental amplifier.

References

[1] A. C. Macpherson, "The center-frequency properties of negative-conductance amplifiers," *IEEE Trans. on Circuit Theory*, vol. CT-11, pp. 136–145, March 1964.
[2] R. D. Hall, "Microwave tunnel diode devices," Sylvania Electric Products, Inc., Electronic Defense Laboratory, Mountain View, Calif., Technical Memorandum EDL-M609, March 20, 1964.
[3] R. M. Aron, "Bandwidth limitations and synthesis procedures for negative resistance and variable reactance amplifiers," California Institute of Technology, Pasadena, Calif., Tech. Rept. 15, August 1960.
[4] L. I. Smilen, "A theory for broadband tunnel diode amplifiers," Rept. Polytechnic Institute of Brooklyn, New York, N. Y., PIBMRI 998-62, April 20, 1962.
[5] E. S. Kuh and J. D. Patterson, "Design theory of optimum negative-resistance amplifiers," *Proc. IRE*, vol. 49, pp. 1043–1050, June 1961.
[6] B. T. Henoch and Y. Kvaerna, "Broadband tunnel diode amplifiers," Stanford Electronics Lab., Stanford Univ., Palo Alto, Calif., Tech. Rept. 213-2, August 1962.
[7] W. J. Getsinger, "Prototypes for use in broadbanding reflection amplifiers," *IEEE Trans. on Microwave Theory and Techniques*, vol. MTT-11, pp. 486–497, November 1963.
[8] J. O. Scanlan and J. T. Lim, "A design theory for optimum broadband reflection amplifiers," *IEEE Trans. on Microwave Theory and Techniques*, vol. MTT-12, pp. 504–511, September 1964.
[9] R. L. Kyhl, R. A. McFarlane, and M. W. P. Strandberg, "Negative L and C in solid-state masers," *Proc. IRE*, vol. 50, pp. 1608–1623, July 1962.
[10] W. H. Ku, "A broad-banding theory for varactor parametric amplifiers," Parts I and II, *IEEE Trans. on Circuit Theory*, vol. CT-11, pp. 50–66, March 1964.
[11] J. O. Scanlan and J. T. Lim, "The effect of parasitic elements on reflection type tunnel diode amplifier performance," *IEEE Trans. on Microwave Theory and Techniques*, vol. MTT-13, pp. 827–836, November 1965.
[12] E. W. Sard, "Analysis of a negative conductance amplifier operated with a nonideal circulator," *IRE Trans. on Microwave Theory and Techniques*, vol. MTT-7, pp. 288–293, April 1959.
[13] D. H. Travena, "Non ideal circulator with negative conductance amplifier," Ferranti Ltd., Wythenshame, Manchester, U. K., Tech. Note 2322, May 1962.
[14] D. W. MacGlashan, "New tunnel diode preamplifier improves phased array radar," *Electronics*, vol. 35, pp. 57–59, September 28, 1962.
[15] J. H. Lepoff, "How to design stable, broadband td amplifiers," *Microwaves*, vol. 3, no. 11, pp. 38–45, November 1964.
[16] R. D. Gallagher, "A microwave tunnel diode amplifier," *Microwave J.*, vol. 8, pp. 62–68, February 1965.
[17] H. M. Wachowski, "A tunable L-band tunnel-diode amplifier," *1961 IRE Internat'l Conv. Rec.*, pt. 3, vol. 9, pp. 64–74, March 1961.
[18] J. Reindel, "A compact tunable tunnel diode S-band receiver," *Microwave J.*, vol. 4, pp. 92–96, December, 1961.
[19] J. Hamasaki, "A low-noise and wide-band Esaki diode amplifier with a comparatively high negative conductance diode at 1.3 Gc/s," *IEEE Trans. on Microwave Theory and Techniques*, vol. MTT-13, pp. 213–223, March 1965.
[20] J. W. Bandler, "Stability and gain prediction of microwave tunnel-diode reflection amplifiers," *IEEE Trans. on Microwave Theory and Techniques*, vol. MTT-13, pp. 814–819, November 1965.
[21] H. J. Butterweck, "Der Y-Zirculator," *Arch. elekt. Übertragungen (Germany)*, Band 17, Heft 4, pp. 163–176, April 1963.
[22] H. Bosma, "On stripline Y-circulation at UHF" *IEEE Trans. on Microwave Theory and Techniques*, vol. MTT-12, pp. 61–72, January 1964.
[23] C. E. Fay and R. L. Comstock, "Operation of the ferrite junction circulator," *IEEE Trans. on Microwave Theory and Techniques*, vol. MTT-13, pp. 15–27, January 1965.
[24] L. K. Anderson, "Broadband circulators for negative resistance amplifiers," presented at Internat'l Conf. at the Microwave Behavior of Ferrimagnetics and Plasmas, London, England, September 1965.
[25] H. W. Bode, *Network Analysis and Feedback Amplifier Design*. Princeton, N. J.: Van Nostrand, 1945.
[26] R. M. Fano, "Theoretical limitations on the broadband matching of arbitrary impedances," *J. Franklin Inst.*, vol. 249, pp. 57–83, 139–154, January and February, 1950.
[27] B. K. Kinariwala, "Realization of broadband matching networks for arbitrary impedances," Electronic Research Laboratory, Univ. of California, Berkeley, Rept. 59, 1957.
[28] D. C. Fielder, "Broad-band matching between load and source systems," *IRE Trans. on Circuit Theory*, vol. CT-8, pp. 138–153, June 1961.
[29] L. Weinberg and P. Slepian, "Takahasi's results on Tchebyscheff and Butterworth ladder networks," *IRE Trans. on Circuit Theory*, vol. CT-7, pp. 88–101, June 1960.
[30] R. Levy, "Explicit formulas for Chebyshev impedance-matching networks, filters and interstages," *Proc. IEE (London)*, vol. 111, pp. 1099–1106, June 1964.
[31] G. L. Matthaei, L. Young, and E. M. T. Jones, *Microwave Filters, Impedance Matching Networks and Coupling Structures*. New York: McGraw-Hill, 1964.

Coupled-Transmission-Line Directional Couplers with Coupled Lines of Unequal Characteristic Impedances

EDWARD G. CRISTAL, SENIOR MEMBER, IEEE

Abstract—A new class of coupled-transmission-line directional couplers, called "nonsymmetrical directional couplers," is described. Unlike conventional directional couplers, nonsymmetrical directional couplers use coupled lines of unequal characteristic impedances. The principal difference between the performance of nonsymmetrical directional couplers and that of conventional designs is the impedance level of the coupled waves, which may be changed to higher or lower impedance levels than that of the incident wave. These directional couplers may be designed to have infinite directivity and to be matched at all frequencies, or they may be designed to have infinite directivity at all frequencies and a specified maximum VSWR. Coupling relationships and design equations for both cases are presented, and the relative properties of both cases are discussed. The theoretical limitation on the maximum coupling and the maximum impedance transformation that can be obtained simultaneously are derived. Techniques for broadbanding by cascading additional sections of coupled lines are described. Experimental results of a trial −10-dB coupler with coupled lines of 50 and 75 ohms are presented.

Manuscript received March 1, 1966; revised April 3, 1966. The work reported in this paper was supported in part by the U. S. Army Electronics Command Laboratories, Fort Monmouth, N. J., under Contract DA 28-043 AMC-01271(E).

The author is with Stanford Research Institute, Menlo Park, Calif.